Computer Simulation of Industrial Low Temperature Shift Reactor for the Purification of Syngas

Fahad M. Alhabdan

Chemical Engineering Department, College of Engineering, King Saud University, P.O. Box 800, Riyadh 11421, Saudi Arabia.

Abstract. A heterogneous one dimensional model for the low temperature shift converter is developed taking into consideration interphase as well as intraparticle mass and heat transfer resistances for the catalyst pellet. The model performance is checked against five industrial reactors in two different plants in Saudi Arabia. The agreement between the model results and the industrial results is very good. The model is used in an application program with the necessary data base for the the physico-chemical parameters. The program is equipped with user friendly input screens with the output obtained as tables and graphs. The package is also equipped with the facility to compute the optimal temperature porofile for constrained and unconstrained optimization. The package can be used for simulation, design and optimization as well as training.

Nomenclature

A	= Cross sectional area of the reactor
b,s	= Subscripts for bulk and surface variables
C	= Concentration of reactants and products.
C_b	= Bulk phase concentration.
C_{ref}	= Reference concentration.
C_p'	= Average molar specific heat.
dp	= Pellet equivalent diameter.
D	= Bulk diffusion coefficient.
D_e	= Effective diffusion coefficient
E	= Activation energy of the reaction.
h	= External heat transfer coefficient.

$(-\Delta H)$ = Heat of reaction.

G = Mass velocity of the gaseous mixture.

k = Rate constant.

k_g, k_e = Mass transfer coefficients.

K = Equilibrium constant.

l = Reactor length coordinate

L = Length of reactor.

M = Molecular weight.

N = Molar flux obeying Fick's Law.

n = Molar flow rate.

N = Nusselt number

$$= \frac{hR_p}{\lambda_e}$$

P = Total pressure

Re = Reynold's Number.

$$= \frac{Gdp}{\mu}$$

R_p = The particle radius

R_G = The Universal gas constant

R = Rate of reaction.

T_b = Temperature of the bulk gas.

T_s = Temperature of the surface of the pellet.

T_{ref} = Reference temperature.

x = Fractional conversion.

X = Mole ratio or dimensionless concentration.
$= (C_A/CA_{ref})$

X_b = Dimensionless bulk phase concentration.
$= (C_{A_b}/C_{ref})$

Y_b = Dimensionless bulk phase temperature.
$= T_b/T_{ref}$

z = Dimensionless depth of reactor.

α $= \dfrac{k\psi A L \exp(-\gamma)}{n_T}$

β = Thermicity factor for the pellet,

$= \dfrac{-\Delta H D_e C_{ref}}{\lambda_e T_{ref}}$

β' = Thermicity factor for the reactor

$= \dfrac{-\Delta H}{C_P T_{ref}}$

γ = Dimensionless activation energy

δ = Diffusibility.

ε = Porosity of the catalyst pellet.

η = The effectiveness factor.

λ_e = Effective thermal conductivity of pellet.

μ = Viscosity of fluid.

ϱ = Density of the gases.

τ = Tortuosity factor.

ϕ = Thiele Modulus.

ψ = Activity factor of the catalyst.

ω = Dimensionless radial distance inside the pellet.

1. Introduction

Shift converters are important gas-solid fixed bed catalyic reactors in the ammonia production lines where the carbon monoxide is treated with steam to produce hydrogen and carbon dioxide, thus purifying the gas from CO and enriching the gas stream with hydrogen [1]. Shift converters are also used in hydrogen production lines to purify the hydrogen before being used in applications such as hydrocracking [2,3, pp. 101-107;4]. The low temperature shift reaction is used as the second process following the high temperature shift reaction, but at lower temperature to insure purification of the gas from CO to about 0.3 – 0.5%

The high temperature shift reactor (HTS) using iron oxide catalyst is used to convert most of the CO to hydrogen and carbon dioxide. However, since high temperature favors high CO content even at equilibrium, the (HTS) effluent still contains about 3% CO. The effluent gases from the (HTS) are usually treated in low

temperature shift reactors (LTS) which uses copper-zinc catalyst and operates in a lower temperature range giving exit gases that contain less than 0.3% CO which is eventually removed in the methanator.

The first commercial application of (LTS) catalyst dates back to 1930 [5]. The catalyst has been subsequently improved and have found widespread commerical application since the early 1960's. The studies on (LTS) are relatively recent [6-13] and are not as exhaustive as that for the (HTS) [14-16]. The simulation study of Singh and Saraf on the low temperature water-gas shift reactor [15] has used a simple rate equation than the one used in this study and also did not solve the diffusion reaction equation for the evaluation of the non-isothermal effectiveness factor. They also did not take into consideration the change of physical properties along the length of the reactor. These factors, especially the simplified rate equation has in many cases resulted in their model over-estimating the CO conversion.

In the present study for the simulation, design, and optimization of these reactors a heterogeneous one dimensional model is developed using a more realastic rate equation than the one used by Singh and Saraf [15]. The model takes into consideration the different resistances associated with the catalyst pellets. The two point boundary value differential equations of the catalyst pellets are solved using the orthogonal collocation method [17]. The resulting model is then coupled with a physical properties to the model. The overall model is solved for the conditions of four industrial reactors and the results of the model are compared with the industrial results.

The model is then used to develop an easy to use reliable computer package simulating the industrial low temperature water gas shift reactors. The software package is user friendly that can be used by a wide spectrum of people in the plant. It can be used in simulation, design, optimization and training as well as for on-line determination of catalyst activity. It is flexible, self contained with graphical capabilities to describe entry and exit conditions.

2. Mathematical Modeling of the Low Temperature Water Gas-Shift Converter (LTS)

The derivation of the mathematical model that describes the performance of the low temperature shift converter (LTS), is presented in the following sections.

Diffusion through catalyst pore represents a considerable resistance to mass and heat transfer, which gives rise to concentration and temperature gradients within the catalyst pellet. This causes the rate of reaction in the solid phase to be different from that obtained where the bulk phase conditions prevail inside the particle, and the average rate of reaction on the pellet should be integrated to get the actual rate of reaction.

The effectiveness factor η is often used in the heterogeneous model to include the external and the intraparticle mass and heat transfer effects [19-22]. The actual

rate of reaction is obtained as the product of η and the rate at bulk conditions.

Heterogeneous models differ from pseudo-homogeneous ones in that the presence of the solid phase and the resistances it offers to both mass and heat transfer are taken into account. Mass and heat balance equations are formulated not only for the bulk of the fluid phase, but also for the solid catalyst phase.

The water gas shift reaction,

$$CO + H_2O \rightleftarrows CO_2 + H_2$$

may be represented by

$$A + B \rightleftarrows C + D$$

where A, B, C, D are CO, H_2O, CO_2, H_2 respectively.

The rate equation used is the one applied by Rase [23] and it was chosen after careful study [23,24,25]. The rate equation is in the form:

$$R = k\psi \frac{(X_A X_B - X_C X_D/K)}{379\,\varrho_b} \quad \frac{\text{lb moles CO reacted}}{\text{(lb catalyst) hr}} \tag{1}$$

Where

k = Rate constant

$= \exp(12.88 - 3340/T)$ T in °R

ψ = Activity factor for the type of catalyst

$= 0.86 + 0.14\,P$ for $P \leq 24.8$

$= 4.33$ for $P > 24.8$ (2)

Multiplying the rate equation by ϱ_b (bulk density of catalyst) to obtain the rate of reaction in units of moles of CO converted per unit volumes of catalyst per seconds, and converting the units to c.g.s. units, the rate equation becomes

$$R = k'\psi(X_A X_B - X_C X_D/K) \quad \frac{\text{g-mole of CO reacted}}{\text{cm}^3 \text{ catalyst sec}} \tag{3}$$

where

$$k' = k_0 e^{-E/RT} \qquad T \text{ in } °K$$

The above pre-exponential factor k_0 includes the diffusion effect as given by the manufacturer [23]. The intrinsic rate constant is obtained as described in [24]. The resulting intrinsic rate constant is used for reactor I. For reactors II, III, and IV, this intrinsic rate constant is modified to account for the change in surface area and operating pressure.

The derivation of the differential equations describing the pellet mass and heat balances is based on the following assumptions:

1- Catalyst particles have a homogeneous porous structure.

2- Mass transfer within the particle of catalyst occurs by diffusion only which may be expressed by means of a constant effective diffusion coefficeint D_e, and the rate of intraparticle diffusion is described by Fick's law.

3- Heat transfer within the particle of catalyst occurs by conduction through the solid portion of the pellets only. It is described by Fourier's law.

4- Both mass and heat transfer inside the catalyst pellet take place in the radial direction only.

A component material blance is made through a shell of thickness (dr) inside the spherical particle. At steady state, the mass balance equation in a dimensionless form is:

$$\nabla^2 X_i = \phi_i^2 \exp(\gamma(1 - 1/Y))R' \qquad (4)$$

where

$$R' = (X_A X_B - X_C X_D/K)$$

and ϕ is Thiele modulus for the pellet defined as:

$$\phi_i = \sqrt{\frac{R_p^2 \psi k_0'}{D_{ei} C_{ref}}}$$

also

$$K' = K_0 \exp(-\gamma)$$

and γ is dimensionless activation energy defines as:

$$\gamma = (E/R_G T_{ref})$$

Equation (4) is a second order differential equation of the boundary value type having two split boundary conditions:

at $\omega = 0$ $\qquad dX_i/d\omega = 0 \qquad (5\text{-a})$

at $\omega = 1$ $\qquad dX_i/d\omega = Sh_i(X_{ib} - X_{is})$ (5-b)

where i = A,B,C,D and $X_{ib} = X_i(\omega = 1)$

The steady state enthalpy balance over the shell of thickness (dr) is given by :

$$\nabla^2 Y_i = -\phi_i^2 \beta_i Exp(\gamma(1 - 1/Y))R' \tag{6}$$

where β_i is the thermicity factor of the pellet for component i defined as:

$$\beta_i = (-\Delta H)D_{ei}C_{ref}/\lambda_e T_{ref}$$

The boundary conditions being:

at $\omega = 0$ $\qquad dY/d\omega = 0$ (7-a)

at $\omega = 1$ $\qquad dY/d\omega = Nu(Y_b - Y_s)$ (7-b)

For a spherical catalyst particle, the non-isothermal effectiveness factor (η) is defined as:

The actual rate of reaction (R)/ Rate of reaction neglecting diffusion resistances (R_B)
In dimensionless form, the above equation becomes:

$$\eta = \frac{\int_0^1 \omega^2 Exp(\gamma(1-1/Y))(X_A X_B - X_C X_D/K)d\omega}{\int_0^1 \omega^2 Exp(\gamma(1 - 1/Y_b))(X_{A_b} X_{B_b} - X_{C_b} X_{D_b}/K_b)d\omega} \tag{8}$$

it can also be written as

$$\eta = (3/R_b)\int_0^1 \omega^2 R d\omega \tag{9}$$

The pellet mass and heat balances are described by second order differential equations of the two point boundary value type. The orthogonal collocation method with one internal collocation point was used to transform the differential equations into a set of nonlinear algebraic equations. Previous investigations have shown that one internal collocation point is adequate to give very accurate results for this problem [26,27]. The resulting set of algebraic equations is reduced to a single non-linear algebraic equation using the well known stoichiometric and heat balance relations (equations 19 and 20). The single non-linear algebraic equation is solved numerically

using the bisectional method [28]. The application of the orthogonal collocation method [17] was also used to provide an algebraic expression for the integral representing the effectiveness factor (η). Thus (η) can be calculated in terms of the dimensionless temperatures Y_1, Y_2 (The details of this is given elsewhere [24]):

$$\eta = [3/F(Y_b)](W_2F(Y_1)+W_2F(Y_2))$$

$$= (0.7\,R_1 + 0.3R_2)/R_b \qquad (10)$$

The heterogeneous model is developed in terms of the bulk variables with the effectiveness factor introduced to account for the diffusional limitations. Certain assumptions has been made for the overall reactor model, these are:

1- Distribution of gas flow velocity inside the converter is uniform.
2. The reactor is studied under adiabatic steady state conditions.
3. Radial distribution of the temperature and concentration of the different components inside the converter are uniform, *i.e.* the model is one-dimensional.
4. Heat and mass diffusion in the longitudinal direction are negligible considering the very high gas velocities at which the reactor is operated, *i.e.* axial dispersion is neglected.
5. Pressure drop across the reactor is negligible compared to the total pressure of the reactor.

At steady state, a component molar balance on CO over an element of catalyst of thickness dl and a cross sectional area (A), with a constant total molar flow rate n_T, gives:

$$dn_A/dl = -\eta\, AR \qquad (11)$$

where n_A is the molar flow rate of component A, and the rate of reaction is given by [23,14]

$$R = k_0\psi \exp(-E/R_G T_b)(X_{A_b}X_{B_b} - X_{C_b}X_{D_b}/K_b) \qquad (12)$$

In a dimensionless form, the equation becomes:

$$dX_{Ab}/dz = -\alpha\,\eta \exp(\gamma(1-1/Y_b))(X_{A_b}x_{B_b} - X_{C_b}X_{D_b}/K_b) \qquad (13)$$

Where K_b is the temperature dependent equilibrium constant which is defined as [23]

$$K_b = \frac{(CO_2)(H_2)}{(CO)(H_2O)}$$

$$= \exp(-4.7+8640/T) \quad T \text{ in } °R \qquad (14)$$

Also $(CO_2),(H_2),(CO),(H_2O)$ are the partial pressures of the different species in equilibrium.

The boundary condition at inlet of reactor is

$$\text{at } l = 0, \quad \text{or} \quad z = 0,$$

$$X_{A_b} = X_{A_f} \tag{15}$$

At steady state, the heat balance equation is:

$$d\Gamma_b/dl = A(-\Delta H)\eta R/n_T \bar{C}_p \tag{16}$$

In a dimensionless form, the equation will be:

$$dY_b/dz = \alpha\,\beta'\eta \exp(1-(1/Y_b))(X_{A_b}X_{B_b} - X_{C_b}X_{D_d}/K_b) \tag{17}$$

The boundary condition is

$$\text{at } z = 0,$$
$$Y_b = Y_f \tag{18}$$

The bulk phase temperature can also be computed from the bulk phase concentration by making cumulative heat balance over the length of reactor (l) to give

$$Y_b = Y_f + \beta'(X_{A_f} - X_{A_b}) \tag{19}$$

Therefore, there is no need to integrate equation (17) along the length of the reactor, equation (19) can be used instead.

The subroutine for the calculation of effectiveness factor is used at each step of the solution to obtain the values for (η), which is substituted in the material balance equation.

From stoichiometry, at any depth of the reactor, the concentrations of CO_2, H_2O, and H_2 can be expressed as functions of the bulk concentration of CO as follows:

$$X_{ib} = X_{if} + a(X_{A_f} - X_{A_b}) \tag{20}$$

where i= B,C,D

The numerical integration of the material balance equation is accomplished by a Runga-Kutta method [28] with variable step size for accuracy. Thus, the axial con-

centration, and temperature profiles are obtained for the shift converter performance, together with variation of the effectiveness factor along the length of the reactor. (*e.g.*: it varies in the range 0.2–0.4).

The instrinsic rate constant is measured for fine powders of the catalyst, and the apparent rate constant is measured for different commercial pellet sizes. Catalyst manufacturers provide rate equations with apparent rate constants including an activity factor which takes into account the effect of pressure and decay. Both the apparent rate constant and the activity factor contain the effect of diffusional limitation. Thus, the computation of the intrinsic rate constant is necessary in order to apply the concept of the effectiveness factor (η) in the heterogeneous model. Therefore, a simple iterative computational algorithm was used to compute the intrinsic rate constant from the reaction rate equation provided by the manufacturer [23]. The procedure is described in [24].

3. Physical Properties Evaluation

An evaluation of the physical properties for the model solution is described, also diffusion coefficients calculation, and external mass and heat transfer coefficients are discussed.

The transport parameters for this model were evaluated using a corresponding state conformal solution procedure [29-31] to predict the transport coefficients of fluids, and mixtures. This is based upon the work of Ely and Hanley [18]. The approach is predictive, and the only input data required are the critical parameters, molecular weight, Pitzer's acentric factor, and for thermal conductivity, the ideal gas specific heat.

The Prandtl number P_r was computed as

$$P_r = \frac{C_p \mu}{\lambda}$$

The binary diffusion coefficient of each component is computed by the simple relation:

$$D_{AB} = \frac{10^{-3}\, T^{1.75} [(M_A + M_B)/ M_A M_B]^{1/2}}{P\left((\sum v_A)^{1/3} + (\sum v_B)^{1/3} \right)^2} \quad \text{cm}^2/\text{sec} \qquad (21)$$

Where v_i are the values of atomic and structural diffusion-volume coefficients [24].

The value of the diffusion of each component in the mixture is calculated by the relation [32]

$$\frac{1 - X_i}{D_{i,mix}} = \sum_{j=1, j \neq i}^{N} \frac{X_j}{D_{i,j}} \tag{22}$$

where

X_i = Mole fraction of each component
$D_{i,j}$ = The binary diffusion coefficient

The simplified relation was found to be adequate for the present simulaiton and optimization study, a more rigorous "dusty-gas" model will complicate the computation without appreciable improvement to justify it.

Correlations for both mass and heat transfer coefficients k_g,h are found empirically from the mass and heat transfer factors J_D and J_H correlations which are defined as:

$$J_D = k_{g_i} \frac{\bar{PM}}{G} (Sc_i)^{2/3} \tag{23}$$

$$J_H = \frac{h}{\bar{C}_p G} (P_r)^{2/3} \tag{24}$$

where

$D_{i,mix}$ = Diffusion coeff. for each component in the mixture

The values for the J_D, J_H are nearly equal and they are computed as functions of the Reynolds numbers (Re)

$$\begin{aligned} J_D \cong J_H &= 0.989\, Re^{-0.41} \quad \text{for} \quad Re > 350 \\ &= 1.820\, Re^{-0.51} \quad \text{for} \quad Re < 350 \end{aligned} \tag{25}$$

where

$$Re = \frac{Gdp}{G\mu} \tag{26}$$

The external mass transfer in the pellet equation takes the form

$$(-N_A) = k_c (C_{A_b} - C_{A_s}) \tag{27}$$

and the external mass transfer coefficient is calculated by this relation:

$$K_{C_i} = K_{g_i} (R_G T) \tag{28}$$

Where T = The average temperature for catalyst bed

The effective diffusion coefficient is computed from the following equation [33]

$$D_{1,2_{off}} = \frac{D_{1\text{-}2}\epsilon}{\tau} = D_{1\text{-}2}\delta \tag{29}$$

where

$D_{1,2_{eff}}$ = The effective bulk diffusion within catalyst

$D_{1\text{-}2}$ = The diffusion coefficient

ε = Porosity of the catalyst pellet

τ = Tortuosity factor

δ = Diffusibility

= 0.041 By experimental investigations [33-35]

For the shift reaction under consideration, the γ,β parameters are equal to 2.97, 0.0104 respectively. Sh, Nu, and ϕ vary along the length of the reactor and from one reactor to another, and the values are in the range, 30-50, 0.25-0.4, 7-10 respectively.

The difference between the temperature at the internal collocation point and the bulk temperature varies with the physico chemical and operating variables, with position of the particle along the length of the reactor and particle size, it is in the range 6-10°C.

4. Computer Program

In the reactor modeling field, most of the commercial packages available to the industry are based on over simplified models or even empirical relations. The presented package is based upon sophisticated heterogeneous model which takes into consideration interphase and intraparticle resistances.

The amount of memory needed for this package is around 195 Kb, and it can be used from a hard disk, or a floppy drive.

The computer program in general is an interactive, easy to use application program with the necessary data base for the physico-chemical parameters, prompting the user for needed information. It is menu driven with choices based upon different types of problems. It is driven by the choices made by the user with the function keys. Most of the screens in the program are graphic based screens with colors. The prog-

ram structure has three distinct sections, namely input, calculation, and output, as shown in Fig. 1.

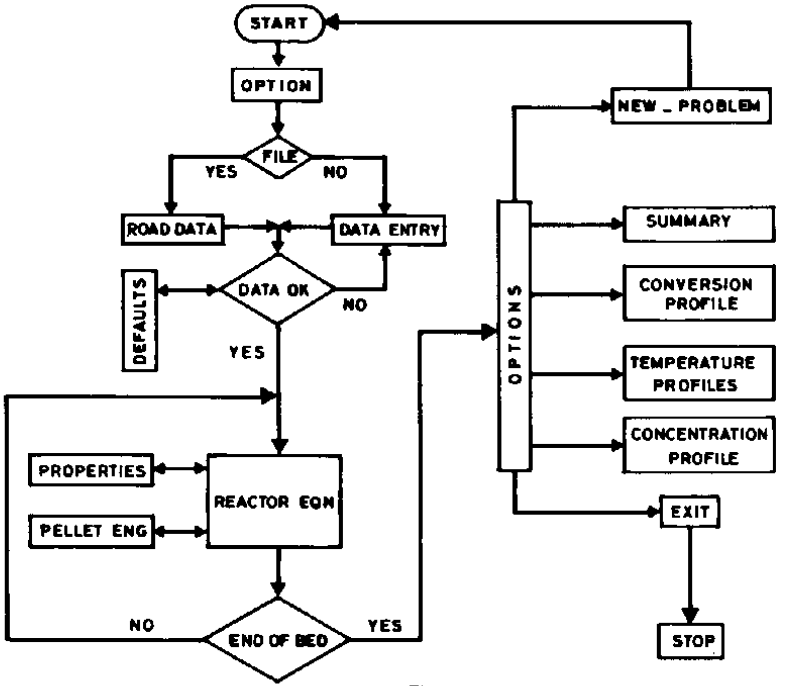

Fig. 1

The input section is for data entry and validation by the user. It starts with the problem type choice which is done through menu selection with the option for reviewing and changing the selection. Once the choice is final, then the data are entered either directly, or through the use of data file which is just an ascii file with required data in sequential order. In the case of direct entry, a screen with fields is presented to the user to fill in the data. The data is verified item by item with the choice of input restriction to a range of values. With the choice of data file, the name of the file is requested and data is read from the file. The data is also validated and error messages are flagged to the user if there is a file error, at which the user can reenter file name or take appropriate action. A verification screen with the data available to the user is presented in order to edit problem input or change program

defaults. The program defaults are made for general use, but it can be modified if one has a better knowledge of the problem in hand. Fig. 1 is a flow chart for the input section.

In the calculation section the program starts by evaluating the physical properties at the feed conditions. With these properties, the program proceeds to solve for the effectiveness factor corresponding to the bulk concentration at the top of the reactor, then solve for the bulk concentration through the bed at the next step, evaluating all other concentrations and temperatures. This procedure continues toward the end of the bed one step at a time. In each step the physical properties are updated through calls to the physical properties routine, and effectiveness factor is computed at each step. After the solution converges, the program proceeds to the next step, each time showing the user intermediate results consisting of bed section, conversion, temperature, carbon monoxide concentration. Also time and number of internal iterations are displayed. At the end, the program proceeds to the output phase.

5. Results and Discussion

In this section the results are discussed for the industrial reactors verifications. The results for the optimum adiabatic feed temperature are discussed. The optimum and constrained optimum temperature profile operation are also computed.

5.1. Industrial Reactors Verifications

The package was tested against five industrial reactors, in two different plants in Saudi Arabia, the specifications of the reactors are listed in Table 1. These reactors are industrially operating reactors with different feed compositions, and different operating conditions. The feedstock is different to each reactor. The catalyst activity depends upon very complex and interacting phenomena, this is discussed in detail in many papers and texts dealing with catalyst activity [26,36-40]. The effect of catalyst type, composition, and structure on the catalyst activity and the implication of these effects on the extent of generality of the model prediction will be discussed in a forthcoming paper. The program was able to simulate these reactors quiet accurately.

The simulation results for the five reactors are given in Table 2. It is clear from these results that simulation results are close to the industrial results. The maximum deviation is less than 0.6% in the exit conversion, and 1.05% in the exit temperature. These deviations are based on plant measurements which have uncertainty higher than these deviations. In two of these reactors, the exit concentration of carbon monoxide could not be measured by plant operators, and reported as traces. Fig. 2 is a temperature profile simulation across the bed for the five reactors mentioned above. Figure 3 is the conversion profile for these reactors.

The quantity of low temperature shift catalyst installed in commercial reactors is generally three to six times greater than the volume required kinetically to achieve

Table 1. Reactors specifications

Reactors	R-I	R-II	R-III	R-IV	R-V
Feed (Moles)					
Carbon Monoxide	1.27	1.74	1.36	1.42	222.62
Water	36.76	33.87	38.08	38.11	4554.8
Carbon Dioxide	10.5	9.21	5.88	5.88	1568.92
Hydrogen	38.03	52.69	53.53	53.53	5353.22
Methane	0.23	2.55	0.99	1.05	36.47
Nitrogen	13.05	0	0	0	1810.96
Argon	0.16	0	0	0	23.07
Reactor					
Temperature	468.661	475.95	473.15	475.15	493.66
Pressure	19.035	23.11	23.11	23.11	22.863
Flow rate	1865	757.975	757.975	757.975	1710
Diameter	274.32	365.8	365.8	365.8	274.32
Depth	1476	304.8	304.8	304.8	1476
Catalyst					
Pellet diam.	0.44091	0.449	0.449	0.449	0.44091
Surface area	35.0	28.95	23.5	23.5	32.7

Table 2. Output values

Reactors	R-I	R-II	R-III	R-IV	R-V
Conversion					
Operation	93.70	88.33	Trace	Trace	95.60
Simulation	94.23	92.57	95.09	95.00	90.31
%dev	–0.57	–4.80	–		5.53
Exit Temp					
Operation	478.00	494.25	490.15	492.15	507.50
Simulation	483.00	495.50	489.10	491.76	512.12
%dev	–1.05	–0.25	0.21	0.08	–0.91

design performance. As a result of this excess volume, low temperature shift catalyst do not show predictable rates of activity decline. As shown in Figure 3, the required conversion is achieved almost at the first half of the bed, with conversion changing slightly through the end of the bed.

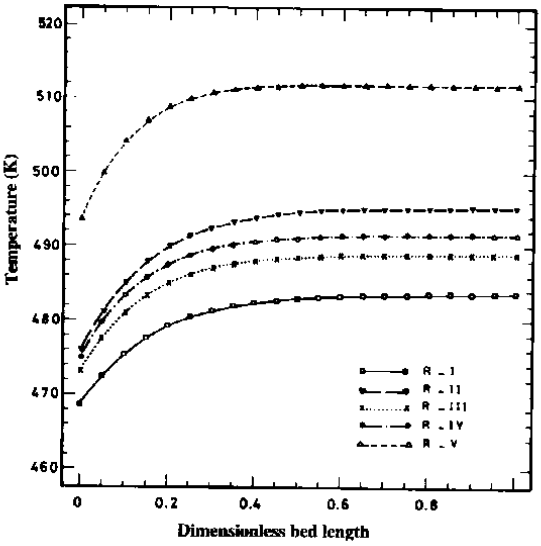
Temperature (K)
520
510
500
490
480
470
460
0
0.2
0.4
0.6
0.8
Dimensionless bed length
R - I
R - II
R - III
R - IV
R - V

Fig. 2

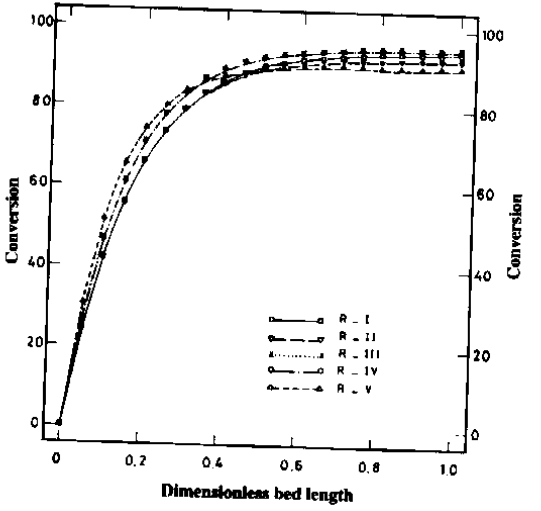
Conversion
100
80
60
40
20
0
0
0.2
0.4
0.6
0.8
1.0
Dimensionless bed length
R - I
R - II
R - III
R - IV
R - V

Fig. 3

5.2. Optimum Feed Temperature for the Adiabatic Reactor

In an adiabatic reactor, and for a certain feed composition, and flow rate, the system can only be controlled through the feed temperature. In an effort to find the optimum adiabatic feed temperature for these operating reactors, with the output conversion as the objective function, the results listed in Table 3 are obtained, the corresponding conversion profiles are plotted in Figure 4. The dimensionless optimum feed temperature ranges between 0.85 to 0.9 of operating feed temperature value. A decrease of feed temperature by 10%, in the case of reactor I, results in an increase of only 2.6% in exit conversion. In the case of reactor II, decreasing the feed temperature by 10%, results in an increase of 8.6% in exit conversion. In the case of reactor V, a decrease of 15%, results in an increase of 1.39% in exit conversion. These results show that these reactors are operating with temperatures higher than the needed optimum. A decrease of operating temperatures results in a higher conversion. The increase of temperature will increase the rate of reaction, but at the same time a decrease in temperature will increase the equilibrium constant, since this reaction is reversible, and exothermic. These competing effects results in the possibility of decreasing the operating temperature with an increase in the exit conversion.

Table 3. Optimum adiabatic feed temperature

Reactors	R-I	R-II	R-III	R-IV	R-V
Temp. (K)					
Operation	478.00	494.25	490.15	492.15	507.50
Optimum Adiabatic	437.48	449.04	442.49	444.98	440.09
T-opt (adiab)/ T-operations	0.90	0.90	0.90	0.90	0.85
Conversion					
Operation	93.70	88.33	Trace	Trace	95.60
Optimum	96.20	95.96	97.30	97.26	96.93
Adiabatic % Increase	2.67	8.64	–	–	1.39

5.3. Optimum Temperature Profile

The optimal temperature profile along the length of the reactor can be obtained through the criterion of choosing the temperature at each point along the length of the reactor, that gives the maximum rate of reaction at this specific point [24]. The mass balance equation of the reactor is given by:

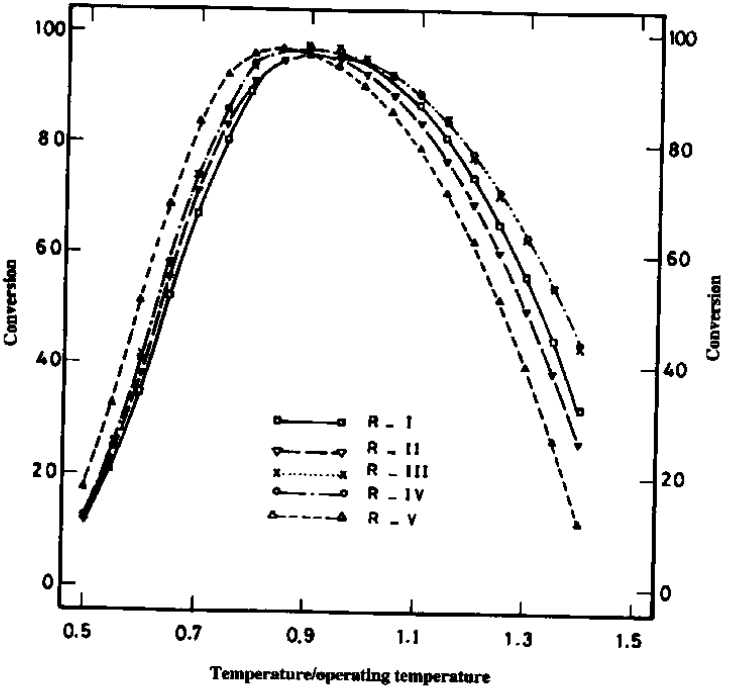

Fig. 4

$$dX_A/dz = -\alpha\eta\exp(\gamma(1-1/Y_b))(X_{A_b}X_{B_b}-X_{C_b}X_{D_b}/K_b) \qquad (30)$$

where

$$K_b = \exp(a + b/Y_b)$$
$$= (-4.72+8640/T) \quad T \text{ in } °R$$

and the X's are fractional conversion. The intrinsic rate of reaction is:

$$r = \alpha\exp(\gamma(1-1/Y_b))(X_{A_b}X_{B_b}-X_{C_b}X_{D_b}/K) \qquad (31)$$

If this rate equation is differentiated with respect to (Y_b), and the derivative set to zero, the optimum value for (Y_b) at each point along the length of the reactor is obtained as:

$$Y_{Optimum} = \frac{b}{In\gamma' - a} \tag{32}$$

Where (γ') varies with the axial position (z) and is given by

$$\gamma' = X_{C_b} X_{D_b} (\gamma + b)/\gamma X_{A_b} X_{B_b} \tag{33}$$

(Note: Rigorously it is $r \cdot \eta$ which should be differentiated with respect to γ_b to obtain the optimum temperature, however this complicates the optimization algorithm considerably without having any appreciable effect on this reactor. This statement can not be generalized since for the ammonia synthesis reactor Elnashaie *et al.* [41] found that optimization with respect to $r \cdot \eta$ improves the performance of the reactor by 3-4%.)

Integration along the length of the reactor gives the optimal temperature profile, and the maximum exit conversion. The optimum temperature profiles were calcualted for the different reactors and the results are given in Table 4, and Figs 5 and 6. The exit conversion increases between 3% to 8% for different reactors, over the operating conversion.

The optimal temperature profiles obtained pose the practical problem of how to implement this optimal temperature policy. The optimal temperature profiles obtained suggest that the reactor should be operated with a relatively high feed temperature followed by very efficient cooling to decrease the temperature sharply at the first 15% of the reactor depth. The implementation of this optimal policy is technically very difficult and very expensive. A number of suboptimal policies were suggested and discussed [27] to overcome the disadvantages of the optimal policy. One of the technical problems associated with optimal temperature is the very high temperature at the reactor inlet part which the catalyst may not be able to withstand.

5.4. Constrained Optimum Temperature Profile

To obtain a realistic optimum condition, a constrain must be imposed upon the maximum allowable catalyst temperature, and other operating and physical limitations. The constrain is in this case taken to be $T \leq 560°K$. The results shown in Table 4, Figures 7 and 8 are obtained for the different reactors. The change in exit conversion decreases by less than 0.5% from the absolute optimum case. This small decrease in exit conversion, is small price for the optimum values to be close to realistic conditions. This policy is obtained through imposing the constraint during the computation of the temperature profile since all points after the constrained portion are dependent upon the results of this portion. This policy can be considered suboptimal with regard to the unconstrained policy.

Table 4. Optimum and constrained optimum values

Reactors	R-I	R-II	R-III	R-IV	R-V
Conversion					
Operation	93.70	88.33	Trace	Trace	85.60
Adiabatic	94.23	92.57	95.09	95.00	90.31
Optimum	97.67	97.30	97.90	98.27	98.13
% Increase over adiabatic	3.65	5.11	2.96	3.44	8.66
Constrained opt.	97.64	97.29	98.30	98.34	98.12
Increase over adiabatic	3.62	5.10	3.38	3.52	8.65
% Change from Optimum	–0.03	–0.01	0.41	0.07	–0.01

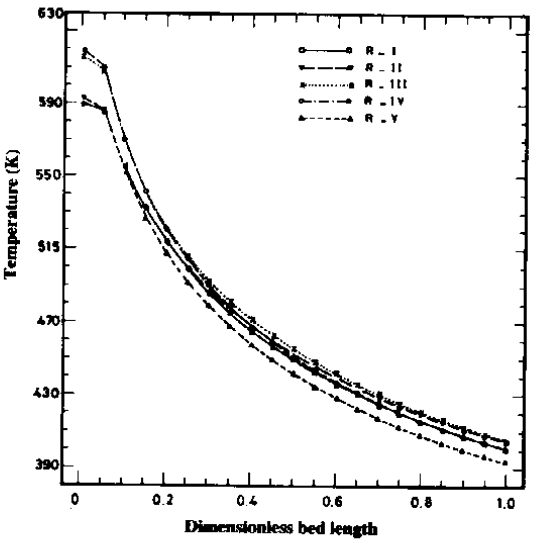

Fig. 5

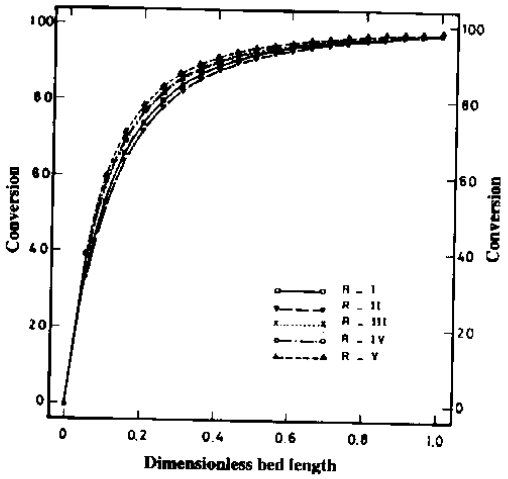
Conversion
Conversion
Dimensionless bed length
R - I
R - II
R - III
R - IV
R - V

Fig. 6

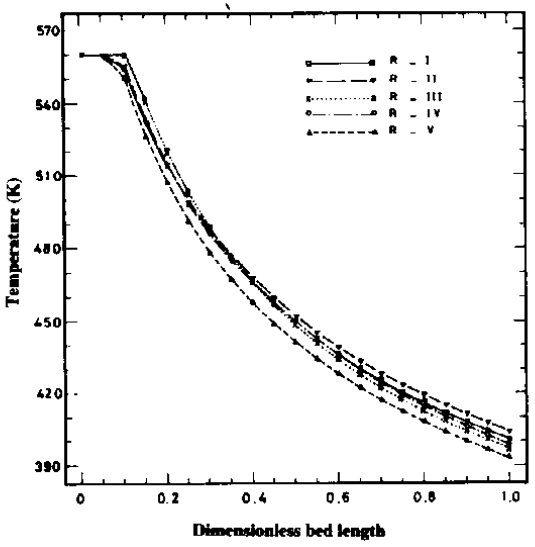
Temperature (K)
Dimensionless bed length
R - I
R - II
R - III
R - IV
R - V

Fig. 7

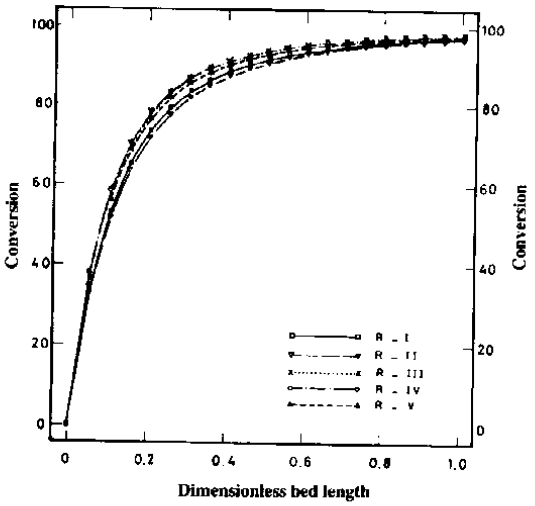

Fig. 8

5.5. Conclusions

The heterogeneous one dimensional model developed and the consideration of the variation of the various physical properties along the length of the reactor given excellent matching with five operating industrial reactors using catalysts which are quite close to each other in composition and activity. The difference between the five reactors with respect to different operating conditions are accounted for in the overall reactor model. The difference in pressure and catalyst specific surface area are accounted for in the effectiveness factor through the Thiele Modulus. To use the model for cases with catalyst of different composition and structure the catalyst activity should be determined experimentally and inserted into the model. The relation between the catalyst activity and its composition and structure is discussed in a forthcoming paper.

The quantity of low temperature shift catalyst installed in commercial reactors is generally three to six times greater than the volume required kinetically to achieve design performance. As a result of this excess volume, low temperature shift catalysts do not show predictable rates of activity decline. In actual practice, the change in bed temperature profile with time is the only reasonable indicator of activity decline. In spite of activity decline in the upper portion of the catalyst bed, the CO slip from a given reactor is maintained very near equilibrium values for prolonged periods of time due to the high activity level of the unaffected portions of the catalyst.

The software package developed on the basis of this model is flexible and is easy to use and suitable for simulation, design, optimization, and training.

The use of the package to study the optimum performance of the reactors shows that optimization based on the adiabatic operation can be achieved only through the manipulation of the feed temperature with a possible improvement over the existing operation of 8%.

The absolute optimum temperature profile gives considerable increase in conversion of all reactors with the maximum increase in conversion of 8.66% occurring for reactor V. Obviously such an operation must be non-adiabatic. The constrained optimal policy that takes into consideration the maximum allowable temperature of the catalyst gives results which are very close to these at the absolute optimum, (*e.g.* increase of conversion over operating conversion of the fourth reactor being 8.6%).

The improvement using non-adiabatic constrained optimal temperature profile are considerable. However for this non-adiabatic operation a two dimensional model for the reactor should be used. The software package is being developed to add the option of using a two-dimensional heterogeneous model for the non-adiabatic case [42].

References

[1] Newsome, D.S. "The Water Gas Shift Reaction." Catal. Rev. Sci. Eng., 21, (1980), 275-318.

[2] Appel, H.R.; Wender, I. and Miller, R.D. "Solubility of Low Rank Coal with Carbon Monoxide and Water," Chem. Ind., London, 47, (1969), 1703-1704.

[3] Thomas, C.I. *Catalytic Process and Proven Catalysts.* New York, USA: Academic Press, 1970.

[4] Weekman, V.W. Jr. "Hydroprocessing Reaction Engineering." Chem. React. Eng. Proc. Int. Symp., (1976), 615-646.

[5] Larson, A.T. *U.S. Patent,* 1797426, (1931).

[6] Borgars, D.J. and Campbell, J.J. "Design and Operation of Co Shift, Naptha and Natural Gas." *Fert. Sci. Technol. S.*, Part 2, (1974), 25-72.

[7] Lambard, J.F. "Cut Sulfur and Chloride: Extend Shift Catalyst Life." *Hydrocarbon Processing,* 48, No. 8, (1969), 11.

[8] Saleta, L.; Such, M. and Vagnerova, V. *Dekturopy,* 9, No. 99 (1969); *Chem. Abstr.* 72, No. 160545 (1970).

[9] Ahmed, S.; Sengupta, A.; Bhattacharya, N.B. and Sen, S.P. *Technology* (India), 8 (1971), 218.

[10] Cherednik, E.M.; Morozov, N.M. and Temkin, M.I. *Kinet. Katal.,* 10, No. 603 (1969), 603.

[11] Kasaoka, S.; Takeda, S.; Sasaoka, E. and Murao, H. "Activity of CuO-Cr_2O_3-ZnO and Fe2O3-Cr2O3 Catalysts for Carbon Monoxide Shift Reaction." *Kogyu Kogaku Zasshi,* 73, No. 1, (1970), 133.

[12] Tsuchimoto, K.; Oda, Y. and Morita, Y., "Rate of Carbon Monoxide Conversions on Copper-Zinc Catalyst." *Kogya Kogaku Zasshi,* 73, No. 1, (1970), 137.

[13] Yureva, T.M. and Boreskov, G.K. *Kinet. Katal.,* 10, No. 603 (1969), 862.

[14] Ruthven, D.M. "The Activity of Commercial Water Gas Shift Catalysts." *Can. J. Chem. Eng.*, 47, (1969), 327.

[15] Singh, C.P.D. and Saraf, D.N. "Simulation of High-Temperature Water-Gas Shift Reactors." *Ind. Eng. Chem. Process Des. Dev.*, 16, (1977), 313.

[16] Alhabdan, F.M. and Elnashaie, S.S. "Digital Simulation of Industrial Shift Converter for the Production of Hydrogen." Accepted *CHEMDATA 88*, Gothenburg, Sweden, June (1988).
[17] Villadsen, J.V. and Michelsen, H.L. *The Solution of Differential Equation Models Using Polynomial Approximation*. London: Prentice Hall, 1978.
[18] Ely, F.J. and Hanley, H.J.M. "Prediction of Transport Properties. 1. Viscosity of Fluids and Mixtures." *Ind. Eng. Chem. Fundam.*, 20 (1981), 323.
[19] Chu, Ci. and Hougen, O.A. "The Effect of Absorbtion on the Effectiveness Factor of Catalyst Pellets." *Chem. Eng. Sci.*, 17 (1962), 167.
[20] Satterfield, C.N. and Roberts, G.W. "Effectiveness Factor for Porous Catalysts." *Ind. Eng. Chem. Fundamentals*, 4 (1965), 288.
[21] Hutchings, J. and Carberry, J.J. "The Influence of Surface Coverage on Catalytic Effectiveness and Selectivity." *A.I.Ch.E. Journal*, 12 (1966), 20-23.
[22] Petersen, E.E.; Merril, R. and John, H.Y. "Effectiveness Factor for Surface Diffusion and Reaction on Catalyst Surface." *Chem. Eng. Sci.*, 25 (1970), 399.
[23] Rase, H.F. *Chemical Reactor Design for Process Plants*. New York, USA: John Wiley, 1977.
[24] Elahwany, A.H. "Simulation and Optimization for an Industrial Shift Converter for the Production of Hydrogen." *Ph.D. Thesis*, Cairo University (1986).
[25] Villadsen, J.V. and Stewart, W.E. "Solution of Boundary Value Problems by Orthogonal Collocation." *Chem. Eng. Sci.*, 22 (1967), 1483.
[26] Elnashaie, S.S.E.H.; Elahwany, A.H. and Elshishini, S.S. "Digital Simulation and Optimization of an Industrial Shift Converter for the Production of Hydrogen I- Reactor Modeling and Simulation." *IASTED Conference*, Cairo, Egypt, 1986.
[27] Elnashaie, S.S.E.H.; Elahwany, A.H. and Elshishini, S.S. "Digital Simulation and Optimization of an Industrial Shift Converter for the Production of Hydrogen II- Optimization." *IASTED Conference*, Cairo, Egypt, 1986.
[28] Rice, J.R. *Numerical Methods, Software and Analysis*. New York, USA: McGraw-Hill, 1983.
[29] Henderson, D.I. and Leonard, J. *Treatise on Physical Chemistry*. New York, USA: Academic Press, VIIIB, 1971, Ch. 7.
[30] Hanly, H.J.M. "Prediction of the Viscosity and Thermal Conductivity Coefficeints of Mixtures" *Cryogenics*, 16, (1976), 634-651.
[31] Evans, D.J. and Hanley, H.J.M. "Viscosity of Mixtures of Soft Spheres." *Phys. Rev.*, A20 (1979), 1648-1654.
[32] Bird, R.B.; Stewart, W.E. and Lightfoot, E.N. *Transport Phenomena*. New York, USA: John Wiley, 1960.
[33] Satterfield, C.N. *Mass Transfer in Heterogeneous Catalysis*. USA: M.I.T. Press, 1970.
[34] Paratella, A. and Guarise, G.B. "Structura Interna di Catalizzatori Porosi e Costante Cinetica Effecttiva." *La Chemica E L'Industria*, 48 (1966), 356.
[35] Hoogschagen, J. "Diffusion in Porous Catalysts and Adsorbents." *Ind. Eng. Chem.*, 47 (1955), 906.
[36] Moss, R.L. "The Structure and Acitvity of Heterogeneous Catalysts." *Chemical Engineer*. (London), (1966), CE114-CE141.
[37] Balz, D.F.; Gettert, H.F. and Gruendler, K.H. "Production of Synthesis Gas by Partial Oxidation and High Pressure Shift Conversion." *Plant/Oper. Prog.*, 2 (1983), 47-79.
[38] Uchida, H.; Isogai, N.; Oba, M. and Hasegawa, T. "Zinc Oxide Copper Catalyst for Carbon Monoxide Shift Conversion. I. Dependency of the Catalyst Activity on The Chemical Composition of the Catalyst." *Bull. Chem. Soc. Jpn.*, 40 (1967), 1981-1986.
[39] Uchida, H.; Isogai, N.; Oba, M. and Hasegawa, T. "Zinc Oxide Copper Catalyst For Carbon Monoxide Shift Conversion. II. Catalyst Activity and the Catalyst Structures." *Bull. Chem. Soc. Jpn.*, 41 (1968), 479-485.
[40] Domka, F. and Wolska, I. "Porous Structure of an Iron(III) Oxide- Thoria Catalyst for the Water Gas Shift Convresion." *Surf. Coat. Technol.*, 28 (1986), 187-200.
[41] Leach, J.W.; Chappelear, R.S. and Leland, T.W. "Use of Molecular Shape Factors in Vapour-Liquid Equilibrium Calculations with the Corresponding States Principle." *AIChE J.*, 14 (1968),

568-579.

[42] Elnashaie, S.S.E.H. and Al-Ubaid, A.S. "Digital Simulation of an Industrial Shift Converter for the Production of Hydrogen." *Modeling and Simulation Conference*, Univ. of Pittsburgh, April (1987).

(*Manuscript Received:* 20.4.1988; *Accepted:* 26.6.1988)

استخدام الحاسب الآلي لمحاكاة مفاعل التحويل ذي الحرارة المنخفضة المستخدم في الصناعة لتنقية غاز التخليق

فهد محمد الهبدان

قسم الهندسة الكيميائية، كلية الهندسة، جامعة الملك سعود، ص.ب ٨٠٠، الرياض١١٤٢١، المملكة العربية السعودية

ملخص البحث. استنباط نموذج أحادي الأبعاد وغير متجانس لمفاعل التحويل ذي الحرارة المنخفضة، وقد أخذ في الاعتبار مقاومة انتقال المادة والحرارة لحبيبات المادة الحافزة سواء فيما بين الطورين أو بداخل الحبيبات.

وقد تمت مواءمة أداء النموذج مع خمس مفاعلات صناعية في مصنعين مختلفين بالمملكة العربية السعودية، وكان التوافق بين النتائج جيدا جدًا.

كما تم استخدام النموذج في برنامج تطبيقي على شكل حزمة مع توفير قاعدة المعلومات الضرورية للمتغيرات الكيميافيزيقية. وقد تم تجهيز البرنامج بشاشات إدخال للمستخدم ليمكن الحصول على النتائج على شكل جداول ومنحنيات كما جهزت الحزمة بالتسهيلات التي تساعد على حساب معدل تغير الحرارة الأمثل في حالتي الأمثلية المشروطة وغير المشروطة كما يمكن استخدام الحزمة في المحاكاة والتصميم. وتعيين الأمثلية، وكذلك للتدريب.